Monatshefte für Chemie - Chemical Monthly
https://doi.org/10.1007/s00706-020-02609-2

ORIGINAL PAPER

Synthesis and biological evaluation of quinoline/cinnamic acid hybrids as amyloid-beta aggregation inhibitors

Yong-Xi Ge[1] · Zhi-Qiang Cheng[1] · Lei Zhou[1] · Hong-Xu Xie[1] · Yin-Yin Wang[1] · Kongkai Zhu[2] · Yang Jiao[3] · Guangpu Liu[4] · Cheng-Shi Jiang[1]

Received: 6 December 2019 / Accepted: 27 April 2020

Abstract

The objective of the current study is to evaluate the potency of quinoline/cinnamic acid hybrids against amyloid-beta (Aβ) aggregation. In total, six new target quinoline/cinnamic acid hybrids were synthesized and screened for their in vitro anti-$A\beta_{42}$ aggregation activity. Some hybrids, including (*E*)-*N*-(2-cinnamamidoethyl)-6,7-dimethoxyquinoline-2-carboxamide, (*E*)-6,7-dimethoxy-*N*-[2-[3-(4-methoxyphenyl)acrylamido]ethyl]quinoline-2-carboxamide, and (*E*)-6,7-dimethoxy-*N*-[2-[3-(2-methoxyphenyl)acrylamido]ethyl]quinoline-2-carboxamide, showed significant anti-$A\beta_{42}$ aggregation activity. Molecular docking method was used to predict the binding modes of these compounds with $A\beta_{42}$. In addition, their cytotoxicity towards neuroblastoma SH-SY5Y and human normal hepatocyte LO2 cells were tested. Neuroprotective evaluation demonstrated that these compounds could attenuate $A\beta_{42}$-induced neurotoxicity towards SH-SY5Y cells in a dose-dependent manner. Overall, the present study provides quinoline/cinnamic acid hybrids as a new template for developing Aβ aggregation inhibitors against Alzheimer's disease.

Graphic abstract

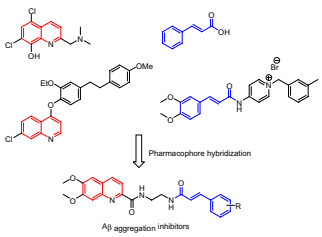

Keywords Quinoline · Cinnamic acid · Aβ aggregation inhibitor · Neuroprotection · Alzheimer's disease

Introduction

Alzheimer's disease (AD) is the most common neurodegenerative disorder, which ranks the third leading death cause after cancer and heart disease. The clinic features of AD usually involves progressive loss of memory and deficits in cognitive functions [1, 2]. The statistic of World Alzheimer Report 2018 shows that about 50 million AD patients were diagnosed worldwide in 2015 and with the aging of global population this number was projected to be 0.15 billion in 2050 [3].

The amyloid beta-peptide (Aβ) deposit is a pathological hallmark of AD and plays a very important role in the

Yong-Xi Ge and Zhi-Qiang Cheng contributed equally to this work.

Electronic supplementary material The online version of this article (https://doi.org/10.1007/s00706-020-02609-2) contains supplementary material, which is available to authorized users.

✉ Guangpu Liu
guang_pu@hotmail.com

✉ Cheng-Shi Jiang
bio_jiangcs@ujn.edu.cn

Extended author information available on the last page of the article

Published online: 12 May 2020

development of AD because of its high propensity for conversion into toxic deposition [4, 5]. Aggregation of Aβ has been identified as a significant factor responsible for cognitive decline and memory deficits in AD [6]. Aβ is a protein consisting of 39–42 amino acids, which can rapidly aggregate to form neurotoxic oligomers, protofibrils, and plaques, consequently leading neuronal cell death. Among these aggregates, the soluble oligomers consisting of $A\beta_{42}$ are the most neurotoxic [7]. Therefore, preventing the aggregation of $A\beta_{42}$ provides a potential approach for AD treatment. As a result, discovering small molecules exhibiting dual inhibitory activity against $A\beta_{42}$ aggregation and neuroprotective effect against $A\beta_{42}$-induced neuronal cell death could be an attractive strategy for R&D of anti-AD drugs [8, 9].

Quinoline is one of the most versatile pharmacophores extensively merging in bioactive molecules against various diseases, including neurodegenerative diseases [10, 11], cancer [12, 13], malaria [14], and inflammation [15]. Various quinoline-based compounds have been also reported to have potential anti-AD activity [16, 17]. One of the quinolone derivatives, 8-hydroxyquinoline derivative PBT2 (a, Fig. 1), could significantly lower cerebrospinal fluid levels of $A\beta_{42}$ and improve cognition, and showed benefits for AD patients in phase II clinical trials [18, 19]. Another quinolone derivative (b, Fig. 1) reported by Hoda et al. also showed potent inhibitory activity against self-mediated, AChE- and Cu^{2+}-induced $A\beta_{42}$ aggregation [20]. In addition, cinnamic acids were also the useful precursors for designing anti-AD molecules due to their ability of endowing derivatives with a variety of pharmacological activities: e.g., antioxidative [21], anti-inflammatory [22], anti-Aβ aggregation [23], and enzyme inhibitory activities [24, 25]. For example, cinnamic acid (c, Fig. 1) could remarkably reduce cerebral $A\beta_{42}$ plaque burden and improve memory of AD mice [23]. Cinnamic acid derivative (d, Fig. 1) exhibited in vitro inhibition on the aggregation of $A\beta_{42}$ and neuroprotective activity against $A\beta_{42}$-induced toxicity in PC12 cells [26].

Molecular hybridization is widely employed as a powerful tool in drug design, which involves the hybridization of different pharmacophores into a single molecular framework to improve pharmaceutical profile [27]. Due to the privileges of quinolone and cinnamic acid, some quinoline/cinnamic acid hybrids were synthesized but mainly for the purpose of antitumor and antimicrobic treatments [28–30], the investigation on their potential for anti-AD treatment has not yet been performed to the best of our knowledge. During our effects to discover new anti-Aβ agents [31–34], six new quinoline/cinnamic acid hybrids **5a**–**5f** (Fig. 1) were recently achieved with chemical agents in hands based on molecular hybridization approach. Herein, we describe the synthesis, in vitro biological evaluation, and molecular docking of this kind of hybrids as anti-$A\beta_{42}$ aggregation and neuroprotective agents.

Results and discussion

Chemistry

Scheme 1 presents the synthetic approach towards these six target hybrids **5a**–**5f**. Briefly, 4,5-dimethoxy-2-nitrobenzoic acid as starting material was treated with iron and acetic acid in refluxing methanol solution to afford 2-amino-4,5-dimethoxybenzoic acid (**1**). The cyclization reaction of **1** with pyruvic acid produced 6,7-dimethoxyquinoline-2-carboxylic acid (**2**). The amidation reaction of cinnamic acids with *tert*-butyl (2-aminoethyl)carbamate yielded (*E*)-*tert*-butyl (2-cinnamamidoethyl)carbamates **3a**–**3f**, which was then deprotected to give *N*-(2-aminoethyl)cinnamamide **4a**–**4f**. Finally, the target (*E*)-*N*-(2-cinnamamidoethyl)-6,7-dimethoxyquinoline-2-carboxamides **5a**–**5f** were prepared from **2** and corresponding (*E*)-*N*-(2-aminoethyl)cinnamamide **4a**–**4f** under amidation condition. The structure of synthesized molecules was confirmed by ^{1}H, ^{13}C NMR, and MS data.

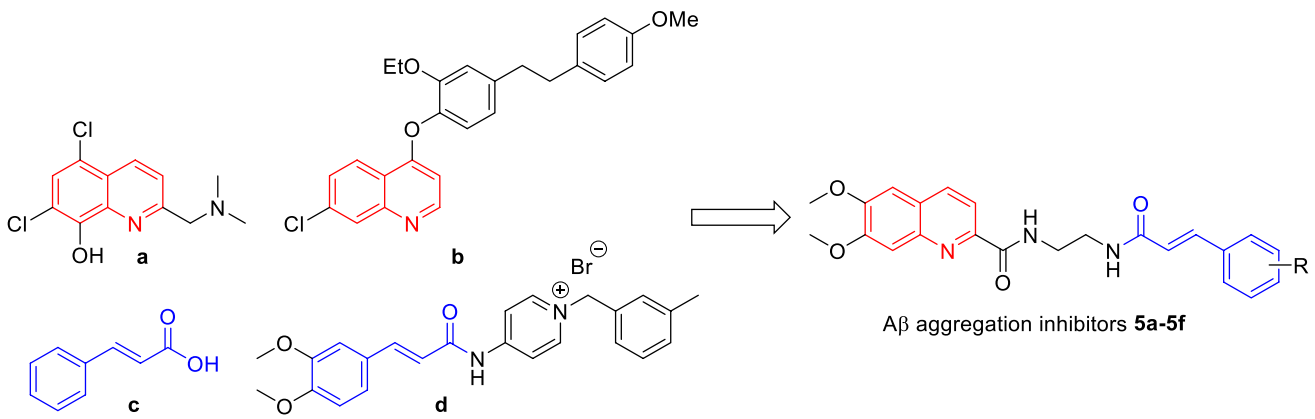

Fig. 1 Design strategy towards new quinoline/cinnamic acid hybrids **5a**–**5f**

Scheme 1

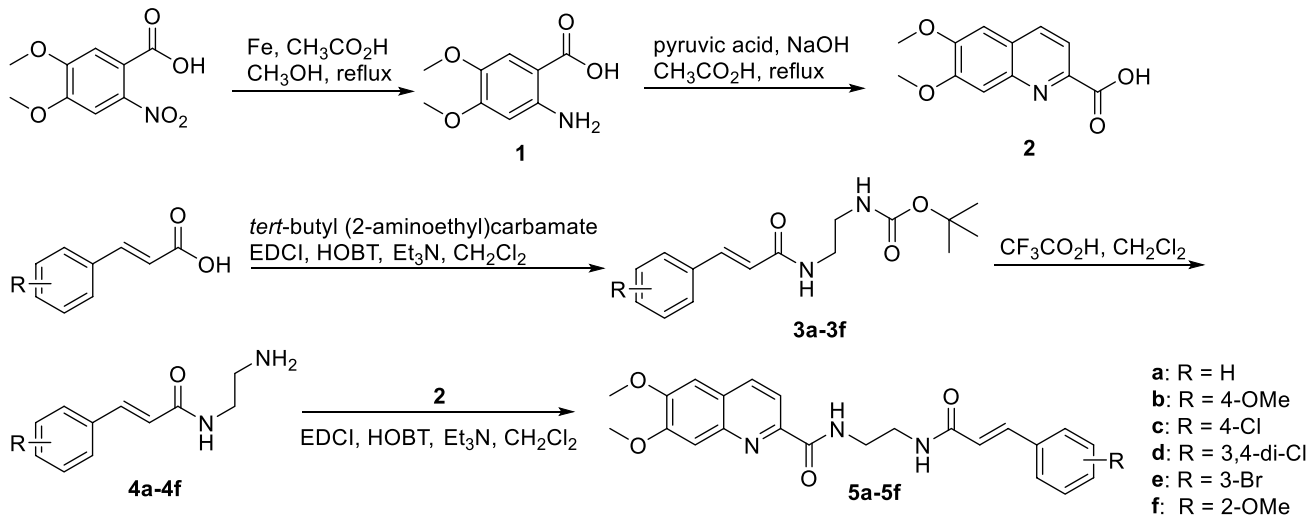

In vitro biological assay

First, all the target compounds were evaluated for their in vitro inhibitory activity against $A\beta_{42}$ aggregation using the thioflavin T (ThT) fluorescence method [35]. Resveratrol was used as a positive control, and galanthamine was taken as a negative control. Their effects on $A\beta_{42}$ aggregation were tested at the concentration of 5–100 μM. As shown in Fig. 2, resveratrol (10 μM) effectively inhibited $A\beta_{42}$ aggregation by 29.5 ± 2.9%, while the negative reference galanthamine shows no significant activity towards $A\beta_{42}$. Among these synthetic hybrids, compounds **5a**, **5b**, and **5f** at 10 μM showed similar anti-$A\beta_{42}$ aggregation activity compared with resveratrol-treated group, and their anti-$A\beta_{42}$ aggregation potency was increased in a dose-dependent manner. The maximal inhibition ratios of **5a**, **5b**, and **5f** against $A\beta_{42}$ aggregation at 100 μM are 67.4 ± 2.8%, 76.3 ± 2.6%, and 62.4 ± 2.5%, respectively. While introducing the electron-withdrawing groups (e.g., Cl or Br) at benzene ring in compounds **5c**, **5d**, and **5e** made the $A\beta_{42}$ aggregation inhibitory activity lose or promoted the aggregation of $A\beta_{42}$. These preliminary results indicated that the electron-donating group at the benzene ring of the cinnamic acid fragment was preferred to increase the inhibitory activity towards $A\beta_{42}$ aggregation.

The $A\beta_{42}$ aggregation could be promoted by the formation of β-sheet structure, thus molecules preventing the formation of a β-sheet structure could have a potential effect for anti-Aβ aggregation [36]. To probe the possible binding modes and key interactions of these compounds with $A\beta_{42}$, the active hybrids **5a**, **5b**, and **5f** were docked to $A\beta_{42}$ monomer (PDB ID: 1IYT) using AutoDock software. As shown in Fig. 3, these compounds interact with $A\beta_{42}$ mainly through hydrophobic interactions with residues, such as Ala21, Val24, Gyl25, Ser26, Asn27, Gly29, and Leu34. In the case of compound **5b**, an intermolecular hydrogen bond interaction is formed between the O atom of carbonyl attached to the quinoline group and the terminal NH_2 group of Lys28, at a distance of 3.12 Å (Fig. 3E). The hydrophobic interactions and a salt bridge between Lys28 and Asp23/Glu22 play an important for stabilizing β-sheet conformational changes in the process of Aβ fibrillogenesis [37]. Based on these

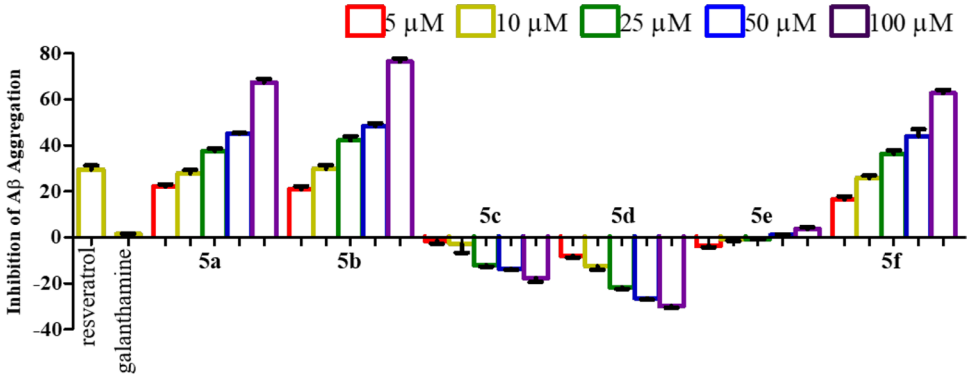

Fig. 2 Inhibition on $A\beta_{42}$ aggregation by hybrids **5a**–**5f** at 5, 10, 25, 50, and 100 μM. Values are express as mean ± SD of three experiments

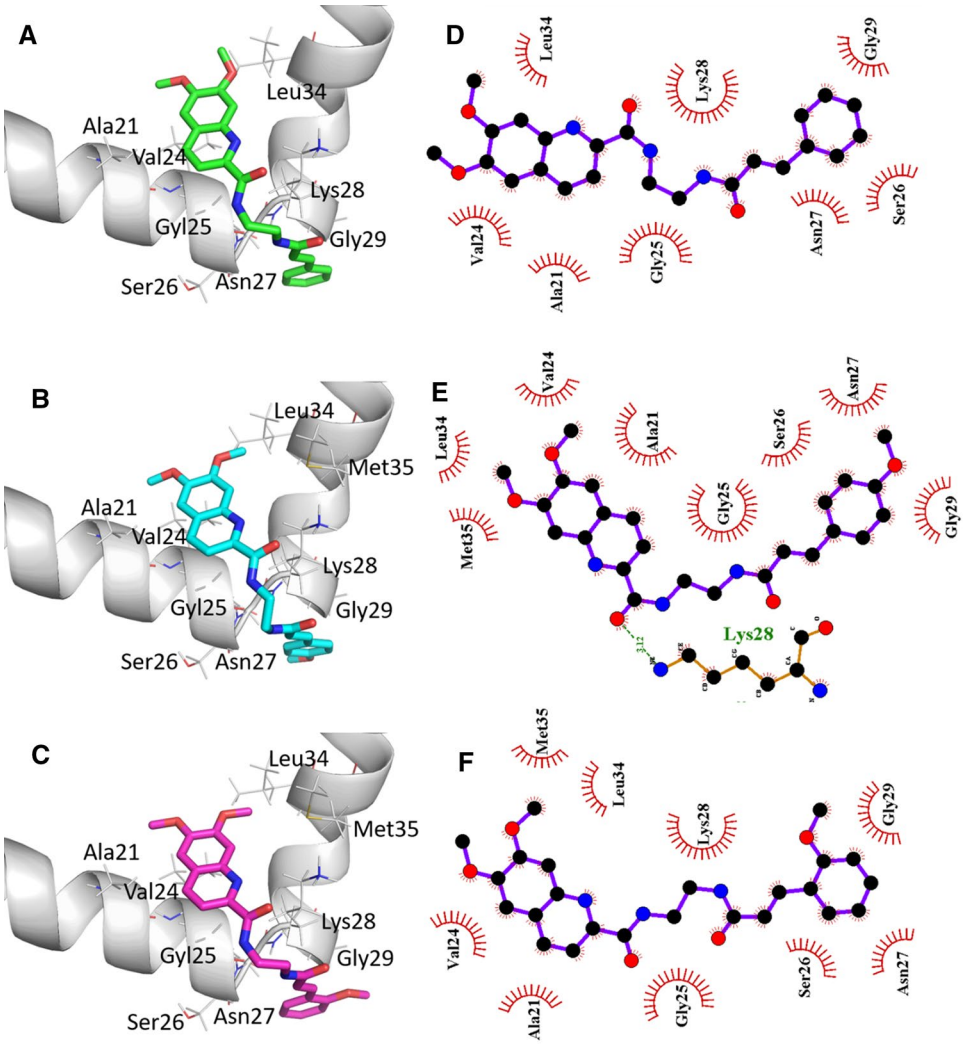

Fig. 3 The predicted binding mode of hybrids **5a**, **5b**, and **5f** with $A\beta_{42}$ (PDB code 1IYT). **a** Compound **5a** (colored green) interacting with $A\beta_{42}$; **b** compound **5b** (colored blue) interacting with $A\beta_{42}$; **c** compound **5f** (colored purple) interacting with $A\beta_{42}$. The relative schematic diagram (**d** for **5a**, **e** for **5b**, **f** for **5f**) showed the hydrophobic interactions (shown as starbursts) and H-bond interaction (denoted by dotted green lines) (color figure online)

molecular docking results, it was proposed that compounds **5a**, **5b**, and **5f** shared a similar binding mode with $A\beta_{42}$ near the stabilizing residues of the α-helix Aβ, and thus inhibited $A\beta_{42}$ aggregation via interfering with the formation of β-sheets.

Since compounds **5a**, **5b**, and **5f** could inhibit the aggregation of $A\beta_{42}$, then their neuroprotective activities against $A\beta_{42}$ aggregation-induced toxicity towards SH-SY5Y neuronal cells were tested. First, the cytotoxicity towards SH-SY5Y cells was evaluated using MTT method [38]. The results shown in Table 1 revealed that all these three compounds have IC_{50} values more than 50 μM. In addition, most of the drugs are metabolized in the liver, and the liver will undergo damage if these drugs are toxic. Therefore, the toxicity of **5a**, **5b**, and **5f** towards human hepatocyte cell line (LO2) was also tested. As shown in Table 1, the IC_{50} of these compounds toward LO2 were in the range of 42.9 ± 1.4 to 60.4 ± 3.1 μM.

Then, the neuroprotective activity of **5a**, **5b**, and **5f** against $A\beta_{42}$-induced neurotoxicity in SH-SY5Y cells was evaluated, with EGCG as a positive reference compound. As shown in Fig. 4, the viability of SH-SY5Y cells was decreased to $63.1 \pm 0.8\%$ by exposed to 10 μM $A\beta_{42}$, while after treated with 10 μM EGCG or synthetic hybrids the viability of SH-SY5Y cells was increased to $85.9 \pm 1.6\%$ (EGCG), $68.2 \pm 1.2\%$ (**5a**), $85.5 \pm 1.1\%$ (**5b**), $79.7 \pm 0.9\%$ (**5f**), respectively, suggesting that these hybrids can stimulate survival of neuroblastoma cells. In addition, the histogram shows these hybrids significantly increasing the SH-SY5Y cell viability in a dose-dependent manner. Among these

Table 1 Toxicity of compounds **5a**, **5b**, and **5f** towards SH-SY5Y and LO2 cells

Compounds	IC_{50}/μM	
	SH-SY5Y	LO2
5a	62.3 ± 1.2	60.4 ± 3.1
5b	70.2 ± 3.4	55.7 ± 2.5
5f	55.8 ± 2.1	42.9 ± 1.4

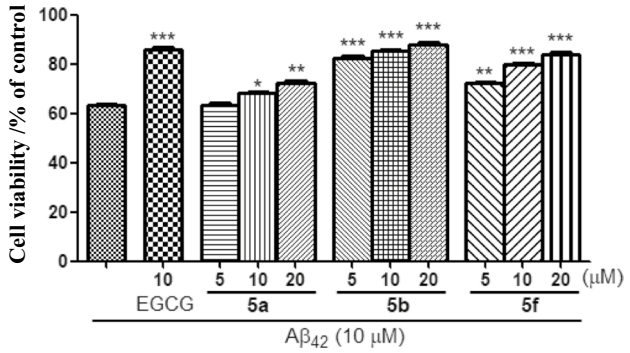

Fig. 4 Neuroprotective effects of compounds **5a**, **5b**, and **5f** against $A\beta_{42}$-induced toxicity in SH-SY5Y cells. Data are expressed as mean ± SD of three experiments. $^{*}P < 0.05$, $^{**}P < 0.01$, $^{***}P < 0.001$ versus $A\beta_{42}$-treated group

compounds, **5b** showed comparable activity to EGCG at both 5 and 10 μM. In general, these results indicated that these compounds could attenuate $A\beta_{42}$-induced neurotoxicity in SH-SY5Y cells.

Conclusion

In summary, six target (*E*)-*N*-(2-aminoethyl)cinnamamides **5a**–**5f** were designed, prepared, and evaluated for their $A\beta_{42}$ aggregation inhibitory and neuroprotective activities. Amongst, compounds **5a**, **5b**, and **5f** could function as new dual anti-$A\beta_{42}$ aggregation and neuroprotective agents. On the basis of results of anti-$A\beta_{42}$ aggregation assay, the electron-donating group at the benzene ring of the cinnamic acid fragment was beneficial for increasing anti-$A\beta_{42}$ aggregation activity. Overall, the present study supports that quinoline/cinnamic acid hybrids could serve as a new template for developing multifunctional anti-AD drug candidates, and continuing investigation into its detailed SAR study and potential for AD treatment is warranted.

Experimental

Commercially available reagents were used without further purification. Organic solvents were evaporated with reduced pressure using a Büchi R-100 evaporator (Büchi, Switzerland). Silica gel column chromatography was performed on Biotage Isolera One (Biotage, Uppsala, Sweden). NMR spectra were measured on Bruker Avance III 600 MHz spectrometer (Bruker, Fällanden, Switzerland). Chemical shifts were expressed in δ (ppm) and coupling constants (J) in Hz with residual solvent signals as standards ($CDCl_3$, $\delta_H = 7.26$ and $\delta_C = 77.2$ ppm; DMSO-d_6, $\delta_H = 2.50$ and $\delta_C = 39.5$ ppm). The purity of the samples was determined by an analytical Agilent 1260 HPLC with ZDRBAX SB-C18 column (4.6 mm × 150 mm) using parameters as follows: H_2O/MeOH, 70/30–0/100 in 15 min, plus 10 min isocratic MeOH, flow rate at 3.0 cm^3/min, $\lambda = 280$ nm. ESI–MS analyses were performed on an Agilent 1260-6460 Triple Quard LC–MS instrument (Agilent, Waldbronn, Germany), and HR-ESI–MS data were acquired on an Agilent 6520 Q-TOF LC/MS (Agilent, Waldbronn, Germany).

2-Amino-4,5-dimethoxybenzoic acid (1) To the mixture of 3.3 g 4,5-dimethoxy-2-nitrobenzoic acid (1 equiv) and 3.5 g iron (4 equiv) in 50 cm^3 CH_3OH was dropwise added 4.5 cm^3 CH_3CO_2H (5 equiv) at room temperature, then the mixture was refluxed for 8 h. The solution was concentrated under reduced pressure, and the obtained residues were purified by flash column chromatography using petroleum ether/ethyl acetate = 2:1 as eluent to give compound **1**. Yield 14.2%; m.p.: 198–200 °C. The NMR analysis was in accordance with previously published data [39].

6,7-Dimethoxyquinoline-2-carboxylic acid (2) Compound **2** was synthesized according to earlier published report [40]. A solution of 400 mg compound **1** (1 equiv), 124 mm^3 pyruvic acid (1.1 equiv), and 486 mg NaOH (5.5 equiv) in 20 cm^3 EtOH was refluxed overnight. Then the solution was acidified to pH ~ 4 by addition of 1 M aqueous HCl at room temperature and then concentrated. The residues was re-crystalized in MeOH to produce **2**. M.p.: 213–215 °C (Ref. [41]: 215 °C). This compound was used in the next step without further purification.

Preparation of compounds 3a–3f and 4a–4f

Compounds **3a**–**3f** and **4a**–**4f** were synthesized according to earlier published protocols [42, 43].

General procedure for the preparation of 5a-5f

To a solution of the corresponding *N*-(2-aminoethyl)cinnamamides **4a**–**4f** (0.21 mmol, 1 equiv) in 5 cm^3 CH_2Cl_2 was added 15 mg HOBT (0.5 equiv), 61 mg EDCI (1.5 equiv), 87 mm^3 Et_3N (3 equiv), and 50 mg compound **2** (1 equiv). The mixture was stirring at room temperature overnight and then concentrated to get residue, which was subject to flash column chromatography to yield target products **5a**–**5f**.

***N*-(2-Cinnamamidoethyl)-6,7-dimethoxyquinoline-2-carboxamide (5a, $C_{23}H_{23}N_3O_4$)** White solid; yield 7.0%; HPLC purity: 96.7%; $t_R = 9.60$ min; ^{1}H NMR (600 MHz, $CDCl_3$): $\delta = 8.57$ (t, $J = 6.0$ Hz, 1H, NH), 8.14 (d, $J = 8.3$ Hz, 1H), 8.11 (d, $J = 8.3$ Hz, 1H), 7.61 (d, $J = 15.8$ Hz, 1H), 7.51–7.47 (m, 2H), 7.37 (s, 1H), 7.36–7.31 (m, 3H), 7.06 (s, 1H), 6.80 (t, $J = 4.4$ Hz, 1H, NH), 6.45 (d, $J = 15.8$ Hz, 1H), 4.04 (s,

3H), 4.03 (s, 3H), 3.78–3.74 (m, 2H), 3.71–3.67 (m, 2H) ppm; ^{13}C NMR (150 MHz, $CDCl_3$): δ = 166.7, 166.6, 153.3, 151.3, 147.1, 143.8, 141.0, 135.5, 135.0, 129.7, 128.9, 128.9, 128.0, 128.0, 125.7, 120.9, 117.4, 107.9, 104.9, 56.3, 56.3, 41.4, 39.4 ppm; MS (ESI): *m*/*z* = 406.0 ([M + H]$^+$); HR-MS (ESI): *m*/*z* calcd for $C_{23}H_{24}N_3O_4^+$ ([M + H]$^+$) 406.1761, found 406.1745.

(*E*)-6,7-Dimethoxy-*N*-[2-[3-(4-methoxyphenyl)acrylamido]-ethyl]quinoline-2-carboxamide (5b, $C_{24}H_{25}N_3O_5$) White solid; yield 20.3%; HPLC purity: 96.5%; t_R = 9.57 min; ^{1}H NMR (600 MHz, $CDCl_3$): δ = 8.56 (brs, 1H, NH), 8.14 (d, *J* = 8.3 Hz, 1H), 8.10 (d, *J* = 8.3 Hz, 1H), 7.56 (d, *J* = 15.3 Hz, 1H), 7.43 (d, *J* = 8.6 Hz, 2H), 7.37 (s, 1H), 7.06 (s, 1H), 6.86 (d, *J* = 8.6 Hz, 2H), 6.68 (brs, 1H, NH), 6.31 (d, *J* = 15.3 Hz, 1H), 4.04 (s, 3H), 4.03 (s, 3H), 3.81 (s, 3H), 3.77–3.72 (m, 2H), 3.70–3.66 (m, 2H) ppm; ^{13}C NMR (150 MHz, $CDCl_3$): δ = 166.9, 166.6, 161.0, 153.3, 151.2, 147.2, 143.8, 140.6, 135.5, 129.5, 129.5, 127.7, 125.7, 118.5, 117.4, 114.3, 114.3, 107.9, 104.9, 56.3, 56.3, 55.5, 41.3, 39.4 ppm; MS (ESI): *m*/*z* = 436.1 ([M + H]$^+$); HR-MS (ESI): *m*/*z* calcd for $C_{24}H_{26}N_3O_5^+$ ([M + H]$^+$) 436.1867, found 436.1876.

(*E*)-*N*-[2-[3-(4-Chlorophenyl)acrylamido]ethyl]-6,7-dimethoxyquinoline-2-carboxamide (5c, $C_{23}H_{22}ClN_3O_4$) White solid; yield 16.2%; HPLC purity: 95.6%; t_R = 11.84 min; ^{1}H NMR (600 MHz, DMSO-d_6): δ = 8.94 (t, *J* = 5.9 Hz, 1H, NH), 8.35–8.31 (m 2H), 7.98 (d, *J* = 15.8 Hz, 1H), 7.58 (d, *J* = 8.5 Hz, 2H), 7.46 (d, *J* = 8.5 Hz, 2H), 7.44–7.41 (m, 3H), 6.63 (d, *J* = 15.8 Hz, 1H), 3.94 (s, 3H), 3.93 (s, 3H), 3.51–3.47 (m, 2H), 3.45–3.41 (m, 2H) ppm; ^{13}C NMR (150 MHz, DMSO-d_6): δ = 165.0, 164.6, 152.9, 150.6, 147.6, 143.0, 137.3, 135.5, 133.9, 129.3, 129.2, 129.2, 129.0, 129.0, 125.0, 123.0, 116.8, 107.4, 105.5, 55.9, 55.7, 38.9, 38.7 ppm; MS (ESI): *m*/*z* = 440.1 ([M + H]$^+$); HR-MS (ESI): *m*/*z* calcd for $C_{23}H_{23}ClN_3O_4^+$ ([M + H]$^+$) 440.1372, found 440.1377.

(*E*)-*N*-[2-[3-(3,4-Dichlorophenyl)acrylamido]-ethyl]-6,7-dimethoxyquinoline-2-carboxamide (5d, $C_{23}H_{21}Cl_2N_3O_4$) White solid; yield 20.4%; HPLC purity: 95.0%; t_R = 14.12 min; ^{1}H NMR (600 MHz, DMSO-d_6): δ = 8.97 (t, *J* = 6.1 Hz, 1H, NH), 8.37–8.31 (m, 2H), 7.98 (d, *J* = 8.3 Hz, 1H), 7.85 (d, *J* = 1.8 Hz, 1H), 7.67 (d, *J* = 8.3 Hz, 1H), 7.56 (dd, *J* = 8.3, 1.8 Hz, 1H), 7.44–7.42 (m, 2H), 7.42 (d, *J* = 15.6 Hz, 1H), 6.69 (d, *J* = 15.6 Hz, 1H), 3.94 (s, 3H), 3.93 (s, 3H), 3.51–3.47 (m, 2H), 3.44–3.42 (m, 2H) ppm; ^{13}C NMR (150 MHz, DMSO-d_6): δ = 164.8, 164.7, 152.9, 150.7, 147.6, 143.1, 136.2, 135.9, 135.6, 131.7, 131.7, 131.1, 129.5, 127.4, 125.0, 124.5, 116.9, 107.5, 105.5, 55.9, 55.8, 38.9, 38.8 ppm; MS (ESI): *m*/*z* = 474.0 ([M + H]$^+$); HR-MS (ESI): *m*/*z* calcd for $C_{23}H_{22}Cl_2N_3O_4^+$ ([M + H]$^+$) 474.0982, found 474.0982.

(*E*)-*N*-[2-[3-(3-Bromophenyl)acrylamido]ethyl]-6,7-dimethoxyquinoline-2-carboxamide (5e, $C_{23}H_{22}BrN_3O_4$) White solid; yield 7.4%; HPLC purity: 95.2%; t_R = 12.44 min; ^{1}H NMR (600 MHz, $CDCl_3$): δ = 8.60 (t, *J* = 6.0 Hz, 1H, NH), 8.13 (d, *J* = 8.5 Hz, 1H), 8.09 (d, *J* = 8.5 Hz, 1H), 7.60 (s, 1H), 7.51 (d, *J* = 15.5 Hz, 1H), 7.43 (d, *J* = 7.5 Hz, 1H), 7.38–7.35 (m, 2H), 7.19 (t, *J* = 6.4 Hz, 1H, NH), 7.07–7.02 (m, 2H), 6.45 (d, *J* = 15.5 Hz, 1H), 4.04 (s, 3H), 4.02 (s, 3H), 3.78–3.73 (m, 2H), 3.71–3.67 (m, 2H) ppm; ^{13}C NMR (150 MHz, $CDCl_3$): δ = 166.7, 166.1, 153.3, 151.3, 147.0, 143.7, 139.3, 137.1, 135.5, 132.5, 130.4, 130.4, 126.7, 125.7, 123.0, 122.4, 117.3, 107.9, 104.9, 56.3, 56.3, 41.4, 39.4 ppm; MS (ESI): *m*/*z* = 484.0, 486.0 ([M + H]$^+$); HR-MS (ESI): *m*/*z* calcd for $C_{23}H_{23}BrN_3O_4^+$ ([M + H]$^+$) 484.0866, 486.0846, found 484.0865, 486.0895.

(*E*)-6,7-Dimethoxy-*N*-[2-[3-(2-methoxyphenyl)acrylamido]-ethyl]quinoline-2-carboxamide (5f, $C_{24}H_{25}N_3O_5$) White solid; yield 6.1%; HPLC purity: 95.2%; t_R = 10.02 min; ^{1}H NMR (600 MHz, $CDCl_3$): δ = 8.56 (t, *J* = 6.2 Hz, 1H, NH), 8.13 (d, *J* = 8.6 Hz, 1H), 8.10 (d, *J* = 8.6 Hz, 1H),7.89 (d, *J* = 15.8 Hz, 1H), 7.46 (dd, *J* = 7.7, 1.6 Hz, 1H), 7.38 (s, 1H), 7.29 (dd, *J* = 7.9, 7.4 Hz, 1H), 7.06 (s, 1H), 6.92 (dd, *J* = 7.7, 7.4 Hz, 1H), 6.88 (d, *J* = 7.9 Hz, 1H), 6.64 (brs, 1H, NH), 6.56 (d, *J* = 15.8 Hz, 1H), 4.04 (s, 3H), 4.03 (s, 3H), 3.84 (s, 3H), 3.77–3.73 (m, 2H), 3.71–3.67 (m, 2H) ppm; ^{13}C NMR (150 MHz, $CDCl_3$): δ = 167.3, 166.4, 158.3, 153.2, 151.2, 147.2, 143.8, 136.5, 135.4, 130.9, 129.0, 125.7, 124.0, 121.6, 120.7, 117.4, 111.2, 108.0, 104.9, 56.3, 56.3, 55.5, 41.0, 39.5 ppm; MS (ESI): *m*/*z* = 436.1 ([M + H]$^+$); HR-MS (ESI): *m*/*z* calcd for $C_{24}H_{26}N_3O_5^+$ ([M + H]$^+$) 436.1867, found 436.1862.

In vitro anti-Aβ aggregation assay

1,1,1,3,3,3-Hexafluoro-2-propanol pre-treated $A\beta_{42}$ (GL Biochem Ltd, shanghai, China) was dissolved in DMSO to make a 200 μM stock solution. The stock solution was centrifuged at the speed of 13,500 rpm for 10 min. The above supernatant was used for further experiments. The compounds for testing were dissolved in DMSO at concentrations of 0.8 mM. A screening assay for the compounds to inhibit Aβ aggregation was performed by measuring ThT fluorescence emission. Compounds (2 mm^3) and 2 mm^3 of 200 μM $A\beta_{42}$ were added into 76 mm^3 of phosphate-buffered saline (PBS at pH 7.4) in a 96-well microtiter plate. After incubation for 24 h at room temperature, 80 mm^3 of 5 μM ThT solution (in 50 mM glycine–NaOH at pH 8.5) was added to the reaction solution. Fluorescence emission was measured at 490 nm with an excitation wavelength of

450 nm on a Tecan Spark multimode microplate reader. The fluorescence intensities were compared and the % inhibition was calculated by the following equation: $100-[(F_i-F_b)/(F_o-F_b)\times 100]$ where F_i, F_o, and F_b are the fluorescence intensities obtained for Aβ aggregation in the presence of inhibitors, $A\beta_{42}$ and ThT; in the presence of $A\beta_{42}$ and THT but no inhibitors; and the blanks containing ThT only.

Molecular docking

The molecular docking studies was performed using AutoDock 4.2, and the amyloid β_{42} structure file (PDB ID: 1IYT) [44] was saved in pdbqt format to perform the docking analysis. The 3D structures of compounds were built and performed MMFF94 minimization using ChemBio3D Ultra 12.0. Using Autodock Tools 1.5.6, preparation of receptor was made by the addition of hydrogen atoms and Gasteiger charges, and final assignment of atomic types as AD4 type, and then autotorsions was used to define the rotatable bonds in the ligand preparation. The resulting enzyme structure was used as an input for the AUTOGRID program. The dimensions of the box were set to $60\times60\times60$ with a grid spacing of 0.375 Å. Rigid ligand docking was performed for the compounds. Docking calculations were carried out using the Lamarckian genetic algorithm (LGA). The proposed docking complex image was created by Pymol 1.5.

In vitro cytotoxicity assay

The SH-SY5Y and LO2 cell lines were cultured in a proper medium supplemented with 10% fetal bovine serum in a humidified atmosphere of 5% CO_2 at 37 °C. Cell suspensions were plated in 96-well plates at a density of 2×10^4 cells/cm^3. Compounds were solubilized in DMSO at six different concentrations, which were then added to each well. After incubation for 24 h, the cells were treated with various concentrations of tested substances for 48 h and then incubated with 10 mm^3 of MTT at 37 °C for 2 h. The formazan dye product was measured by the absorbance at 490 nm on a Tecan Spark multimode microplate reader (Switzerland).

In vitro neuroprotective activity evaluation

SH-SY5Y cells were maintained at 37 °C in a humidified atmosphere containing 5% CO_2. Cells were seeded into multi-well plates at a density of $2–2.5\times10^5$ cells/mm^3 in DMEM medium, supplemented with 10% heat-inactivated bovine calf serum (Gibco, South America Origin). Experiments were carried out in 24 h after cells were seeded. $A\beta_{42}$ were stored at 4 °C until 0.1 mM stock solutions were prepared in phosphate buffer saline (PBS) on the day of application to cultures. The compounds were first dissolved with DMSO and then diluted with DMEM medium. After pretreatment with the compounds for 2 h, $A\beta_{42}$ were added to SH-SY5Y cell cultures in 24 h. Assays for cell viability were performed in 24 h after cultured in fresh medium.

Acknowledgements This research work was financially supported by the Natural Science Foundation of China [no. 21672082], Natural Science Foundation of Shandong Province [nos. ZR2019YQ31, ZR2017BC101], and Shandong Talents Team Cultivation Plan of University Preponderant Discipline [no. 10027].

References

1. Wiemann J, Loesche A, Csuk R (2017) Bioorg Chem 74:145
2. Mattila J, Soininen H, Koikkalainen J, Rueckert D, Wolz R, Waldemar G, Lötjönen J (2012) J Alzheimer's Dis 32:969
3. World Alzheimer Report 2018. https://www.alz.co.uk/research/world-report-2018. Accessed 27 Nov 2019
4. Lorenzo A, Yuan M, Zhang Z, Paganetti PA, Sturchler-Pierrat C, Staufenbiel M, Mautino J, Vigo FS, Sommer B, Yankner BA (2000) Nat Neurosci 3:460
5. Chen GF, Xu TH, Yan Y, Zhou YR, Jiang Y, Melcher K, Xu HE (2017) Acta Pharmacol Sin 38:1205
6. Glabe C (2010) Biophys J 98:3a
7. Selkoe DJ (2001) Physiol Rev 81:741
8. Thorsett ED, Latimer LH (2000) Curr Opin Chem Biol 4:377
9. Ahmad A, Ali T, Park HY, Badshah H, Rehman SU, Kim MO (2017) Mol Neurobiol 54:2269
10. Czaplinska B, Spaczynska E, Musiol R (2018) Med Chem 14:19
11. Van Hau T, Ruankham W, Suwanjang W, Songtawee N, Wongchitrat P, Pingaew R, Prachayasittikul V, Prachayasittikul S, Phopin K (2019) Chem Res Toxicol 32:2182
12. Bayat M, Safari F, Nasri S, Hosseini FS (2019) Monatsh Chem 150:703
13. Lien VT, Olberg DE, Hagelin G, Klaveness J (2019) Monatsh Chem 150:1947
14. Pinheiro LCS, Feitosa LM, Gandi MO, Silveira FF, Boechat N (2019) Molecules 24:E4095
15. Upadhyay KD, Dodia NM, Khunt RC, Chaniara RS, Shah AK (2019) Chem Biol Drug Des 94:1647
16. Huang W, Liang M, Li Q, Zheng X, Zhang C, Wang Q, Tang L, Zhang Z, Wang B, Shen Z (2018) Eur J Med Chem 177:247
17. Mo J, Yang H, Chen T, Li Q, Lin H, Feng F, Liu W, Qu W, Guo Q, Chi H, Chen Y, Sun H (2019) Bioorg Chem 93:103310
18. Faux NG, Ritchie CW, Gunn A, Rembach A, Tsatsanis A, Bedo J, Harrison J, Lannfelt L, Blennow K, Zetterberg H, Ingelsson M, Masters CL, Tanzi RE, Cummings JL, Herd CM, Bush AI (2010) J Alzheimers Dis 20:509
19. Lannfelt L, Blennow K, Zetterberg H, Batsman S, Ames D, Harrison J, Masters CL, Targum S, Bush AI, Murdoch R, Wilson J, Ritchie CW (2008) Lancet Neurol 7:79779
20. Umar T, Shalini S, Raza MK, Gusain S, Kumar J, Ahmed W, Tiwari M, Hoda N (2018) MedChemComm 9:1891
21. Sova M (2012) Mini Rev Med Chem 12:749
22. Takeda Y, Tanigawa N, Sunghwa F, Ninomiya M, Hagiwara M, Matsushita K, Koketsu M (2010) Bioorg Med Chem Lett 20:4855
23. Chandra S, Roy A, Jana M, Pahan K (2019) Neurobiol Dis 124:379
24. Chen Y, Zhu J, Mo J, Yang H, Jiang X, Lin H, Gu K, Pei Y, Wu L, Tan R, Hou J, Chen J, Lv Y, Bian Y, Sun H (2018) J Enzyme Inhib Med Chem 3:290
25. Takao K, Toda K, Saito T, Sugita Y (2017) Chem Pharm Bull (Tokyo) 65:1020

26. Lan JS, Hou JW, Liu Y, Ding Y, Zhang Y, Li L, Zhang T (2017) J Enzyme Inhib Med Chem 32:776
27. Ivasiv V, Albertini C, Gonçalves AE, Rossi M, Bolognesi ML (2019) Curr Top Med Chem 19:1694
28. Pérez B, Teixeira C, Gut J, Rosenthal PJ, Gomes JR, Gomes P (2012) ChemMedChem 7:1537
29. Mabeta P, Pavić K, Zorc B (2018) Acta Pharm 68:337
30. Pérez BC, Teixeira C, Figueiras M, Gut J, Rosenthal PJ, Gomes JR, Gomes P (2012) Eur J Med Chem 54:887
31. Jiang CS, Ge YX, Cheng ZQ, Wang YY, Tao HR, Zhu K, Zhang H (2019) Molecules 24:E2568
32. Jiang CS, Ru T, Yao LG, Miao ZH, Guo YW (2019) Fitoterapia 136:104176
33. Cheng ZQ, Song JL, Zhu K, Zhang J, Jiang CS, Zhang H (2018) Mar Drugs 16:E293
34. Jiang CS, Ge YX, Cheng ZQ, Song JL, Wang YY, Zhu K, Zhang H (2019) J Comput Aided Mol Des 33:521
35. Fang L, Fang X, Gou S, Lupp A, Lenhardt I, Sun Y, Huang Z, Chen Y, Zhang Y, Fleck C (2014) Eur J Med Chem 76:376
36. Meena P, Manral A, Nemaysh V, Saini V, Siraj F, Luthra PM, Tiwari M (2016) RSC Adv 6:104847
37. Rodriguez MH, Morales LGF, Basurto JC, Hernandez MCR (2018) Molecular docking and molecular dynamics simulation to evaluate compounds that avoid the amyloid beta 1–42 aggregation. In: Roy K (ed) Computational modeling of drugs against Alzheimer's disease. Neuromethods, vol 132. Humana Press, New York, p 229
38. Mei WW, Ji SS, Xiao W, Wang XD, Jiang CS, Ma WQ, Zhang HY, Gong JX, Guo YW (2017) Monatsh Chem 148:1807
39. Kopchuk DS, Nikonov IL, Khasanov AF, Giri K, Santra S, Kovalev IS, Nosova EV, Gundala S, Venkatapuram P, Zyryanov GV, Majee A, Chupakhin ON (2018) Org Biomol Chem 16:5119
40. Ge YH, Wu YM, Xuw ZJ (2005) Huaxue Shiji 27:415
41. Walther B, Walter R (1943) Justus Liebigs Ann Chem 554:269
42. Li L, Li Z, Liu M, Shen W, Wang B, Guo H, Lu Y (2015) Molecules 21:E49
43. Li H, Li M, Xu R, Wang S, Zhang Y, Zhang L, Zhou D, Xiao S (2019) Eur J Med Chem 163:560
44. Crescenzi O, Tomaselli S, Guerrini R, Salvadori S, D'Ursi AM, Temussi PA, Picone D (2002) Eur J Biochem 269:5642

Affiliations

Yong-Xi Ge[1] · Zhi-Qiang Cheng[1] · Lei Zhou[1] · Hong-Xu Xie[1] · Yin-Yin Wang[1] · Kongkai Zhu[2] · Yang Jiao[3] · Guangpu Liu[4] · Cheng-Shi Jiang[1]

[1] School of Biological Science and Technology, University of Jinan, Jinan 250022, China

[2] Shandong Key Laboratory of Biochemical Analysis, College of Chemistry and Molecular Engineering, Qingdao of University of Science and Technology, Qingdao 266042, China

[3] Shandong Institute for Food and Drug Control, Jinan 250012, China

[4] Department of Pharmacy, Qilu Hospital of Shandong University, Jinan 250012, China